



Validation of ASTEC V2 models for the behaviour of corium in the vessel lower head

Laure Carénini, Joëlle Fleurot, Florian Fichot

► To cite this version:

Laure Carénini, Joëlle Fleurot, Florian Fichot. Validation of ASTEC V2 models for the behaviour of corium in the vessel lower head. Nuclear Engineering and Design, 2014, 272, pp.152-162. 10.1016/j.nucengdes.2013.06.041 . hal-02614036

HAL Id: hal-02614036

<https://hal.science/hal-02614036>

Submitted on 2 Jun 2023

HAL is a multi-disciplinary open access archive for the deposit and dissemination of scientific research documents, whether they are published or not. The documents may come from teaching and research institutions in France or abroad, or from public or private research centers.

L'archive ouverte pluridisciplinaire **HAL**, est destinée au dépôt et à la diffusion de documents scientifiques de niveau recherche, publiés ou non, émanant des établissements d'enseignement et de recherche français ou étrangers, des laboratoires publics ou privés.



Distributed under a Creative Commons Attribution - NonCommercial - NoDerivatives 4.0 International License

VALIDATION OF ASTEC V2 MODELS FOR THE BEHAVIOUR OF CORIUM IN THE VESSEL LOWER HEAD

L. Carénini*, J. Fleurot, F. Fichot

Institut de Radioprotection et de Sûreté Nucléaire (IRSN), PSN-RES/SAG, Cadarache, Saint-Paul-lez-Durance, 13115, France

* Corresponding author email address: laure.carenini@irsn.fr

ABSTRACT

The paper is devoted to the presentation of validation cases carried out for the models describing the corium behaviour in the "lower plenum" of the reactor vessel implemented in the V2.0 version of the ASTEC integral code, jointly developed by IRSN (France) and GRS (Germany). In the ASTEC architecture, these models are grouped within the single ICARE module and they are all activated in typical accident scenarios. Therefore, it is important to check the validity of each individual model, as long as experiments are available for which a single physical process is involved. The results of ASTEC applications against the following experiments are presented: FARO (corium jet fragmentation), LIVE (heat transfer between a molten pool and the vessel), MASCA (separation and stratification of corium non miscible phases) and OLHF (mechanical failure of the vessel). Compared to the previous ASTEC V1.3 version, the validation matrix is extended. This work allows determining recommended values for some model parameters (e.g. debris particle size in the fragmentation model and criterion for debris bed liquefaction). Almost all the processes governing the corium behaviour, its thermal interaction with the vessel wall and the vessel failure are modelled in ASTEC and these models have been assessed individually with satisfactory results. The main uncertainties appear to be related to the calculation of transient evolutions.

1. INTRODUCTION

ASTEC is an integral code jointly developed by IRSN (France) and GRS (Germany) to simulate the whole sequence of a severe accident in nuclear power plants, from the initiating event up to the fission products releases and their behaviour in the containment, and finally to appreciate radioactive releases out of the containment. The "lower plenum" models implemented in ASTEC deal with the corium behaviour in the reactor vessel from its slump from the central part of the core, its possible fragmentation and solidification in water present in the lower plenum, up to the possible failure of the vessel lower head, taking into account the corium stratification (separation of chemical phases) and heat transfers with the vessel lower head wall. The adequate representation of all of these phenomena should in principle allow an accurate determination of the time of vessel rupture and the characteristics (temperature, composition...) of corium which would flow subsequently in the reactor pit, leading to molten-core-concrete-interaction (MCCI).

Between V1.3 and V2.0 versions of ASTEC, improvements were made on the lower plenum corium models. In particular, a new phase separation model was developed for situations involving a U-Zr-O-Fe molten pool in the lower head (separation between non-miscible metallic and oxide phases) in agreement with MASCA experiments (see Section 5). In addition, the validation matrix of lower plenum

models was also extended (compared to V1.3 version) by adding the LIVE L6 experiment (Table 1). For the six experiments concerned, the results obtained with the V2.0 version are presented and compared with those obtained with the V1.3 version, when existing. The main remaining limitations of the models are also underlined.

Table 1: Validation matrix for lower plenum models of ASTEC

Experiment		Main phenomena	ASTEC V1.3	ASTEC V2.0
FARO	L14	Corium fragmentation	x	x
	L28			
LIVE	L1	Thermal exchanges between the corium molten pool and the vessel	x	x
	L6		-	x
MASCA (STFM/MA series)		Oxide/metal layers stratification	-	x
OLHF-1		Vessel lower head failure	x	x

2. ASTEC MODELLING OF THE CORIUM BEHAVIOUR IN THE VESSEL LOWER PLENUM

In case of reactor calculations performed with the ASTEC code, when the molten corium relocates from the core down to the lower plenum, the melt jets interact with water and may be totally or partially fragmented depending on the level of water inside the vessel. The code evaluates the jet break-up length and deduces the fragmentation rate and the associated water vaporization. Accurate evaluation of this steam production is important in order to be able to predict the associated pressurisation. If the melt jet is totally fragmented, a debris bed is created at the bottom of the lower plenum, but if it is only partially fragmented, a corium layer is formed at the bottom, covered by the debris bed (Fig.1). Then ASTEC evaluates the separation of non-miscible liquid oxide and metal phases and the stratification of those phases up to 3 corium layers. Heat transfers are evaluated between all the layers in the lower plenum as well as between corium and the vessel wall and the internal structures. A specific model is also available to take into account the focusing effect related to the formation of a thin metallic layer. In that case, the layer thickness is small compared to the vessel mesh size in contact, which requires a particular treatment to calculate accurately the significant heat flux at that location. Models are implemented to take into account the possible melting of the debris layers, which then feed the corium layers, and the sinking of debris into corium layers or inversely, depending on their relative density and viscosity. When the vessel wall heats up, its mechanical deformation and progressive melting are calculated until its possible failure.

All these models allow to calculate the timing and mode of vessel failure, as well as the properties of corium which will flow out of the vessel. These properties will impact phenomena like steam explosion, MCCI and direct containment heating (DCH) in the containment.

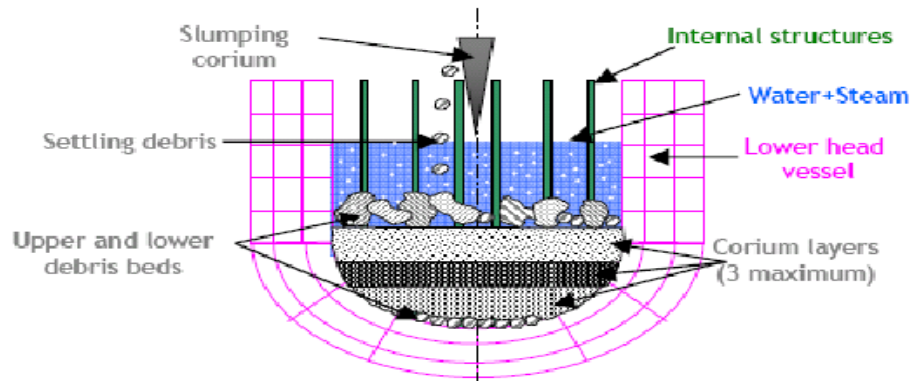


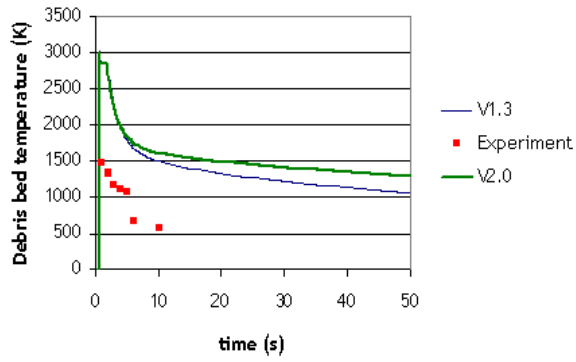
Fig.1 – Schematic representation of the corium behaviour in the vessel lower plenum as implemented in the ASTEC code

3. ASTEC VALIDATION VS. FARO EXPERIMENTS

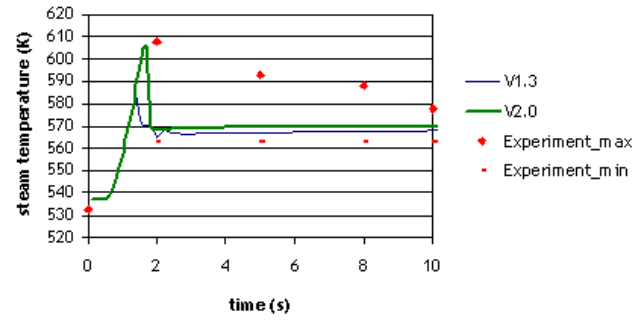
The FARO-L14 and FARO-L28 experiments, performed by JRC-Ispra (Italy), were designed to study the interaction of a corium melt (80 wt% UO_2 , 20 wt% ZrO_2) poured by gravity into a pool of water at saturation temperature. More information about L14 and L28 tests is available in Magallon et al. (1997) and Magallon (2006).

3.1. Comparison of ASTEC V1.3 and V2.0 results

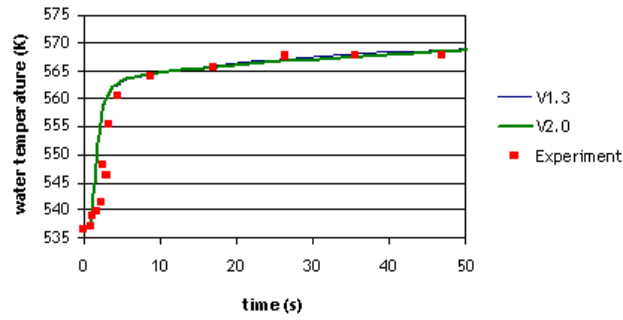
The L14 and L28 experiments have already been simulated with the V1.3 version of ASTEC (Bandini et al., 2010). Thus the same modelling has been considered for the V2.0 calculations. It uses the ICARE module for the vessel phenomena, coupled with the CESAR module for the circuit thermal-hydraulics (in particular for annular space simulation in L28 test). With the V1.3 version the best results were obtained considering a diameter of 3.5 mm for the debris formed by fragmentation for the L14 test and 3 mm for the L28 test assuming spherical particles. These values are in accordance with the range of particle diameters observed experimentally (see Magallon, 2006). The same parameters have been chosen for comparison with the V2.0 version. The results are presented in Fig.2 and Fig.3 and compared with the available data for both experiments.



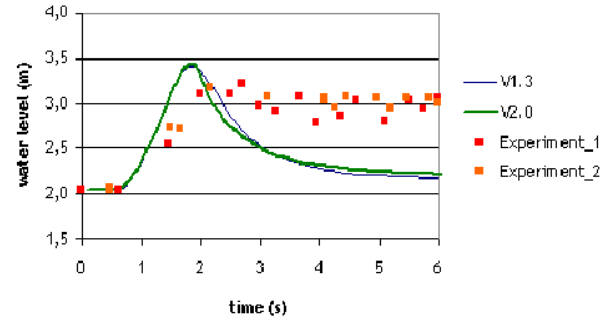
a)



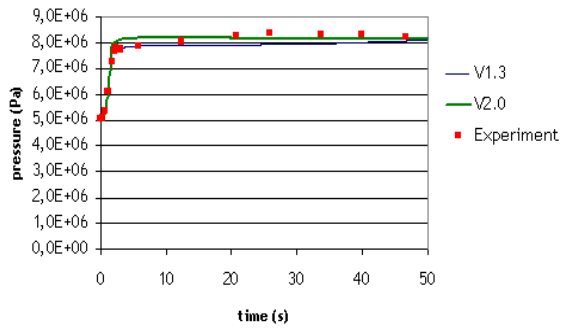
b)



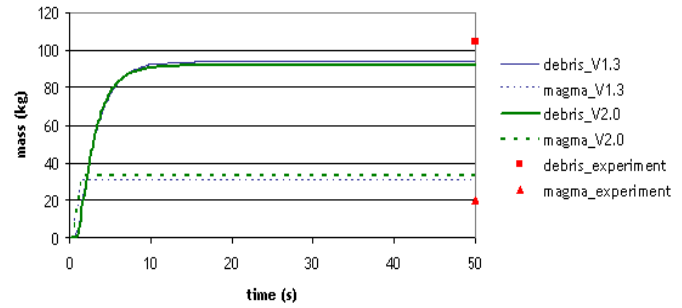
c)



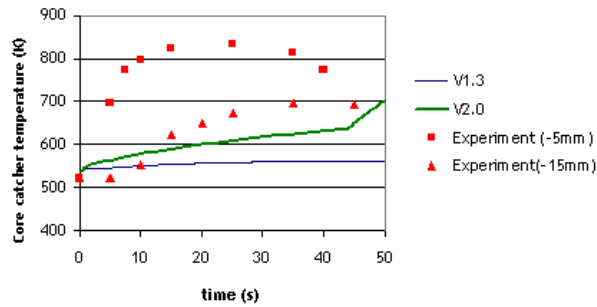
d)



e)



f)

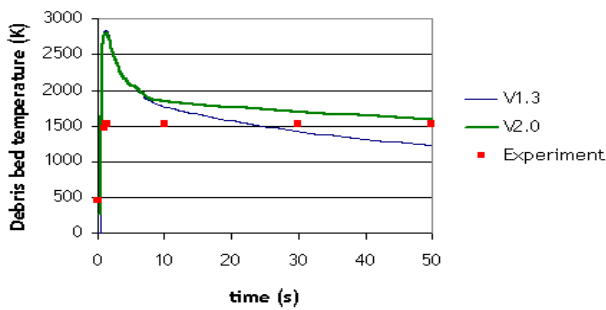


g)

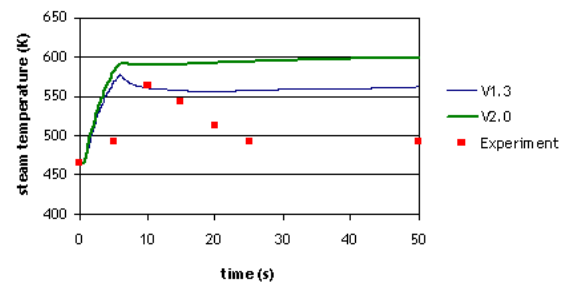
Fig.2 - L14 experiment : a) masses (the melt is named “magma”), b) pressure history, c) water level, d) water temperature, e) steam temperature, f) debris bed temperature, g) core catcher temperature

For the L14 experiment, the differences between V1.3 and V2.0 calculations are significant only for the core catcher temperature and might be due to a correction made in V2.0 on the evaluation of the conductivity of the debris bed taking into account its porosity. The evolution of the main parameters of the experiment is well reproduced. In particular, there is a very good agreement on pressure elevation and water and steam temperatures. The remaining discrepancies are:

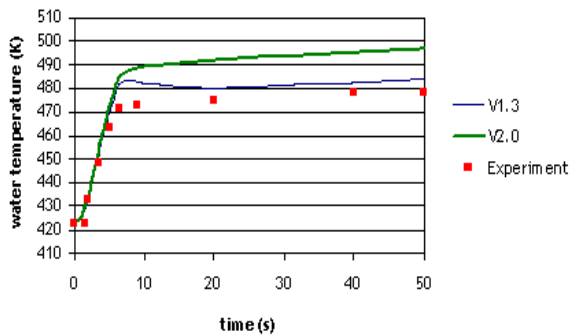
- The fraction of fragmented corium: almost 74% in the calculation, whereas the experimental data is 84%;
- The period of time during which the water level is maintained high: this could be related to an underestimation of water boiling;
- The debris bed temperature: this discrepancy could be explained by the one observed on water level, showing an underestimation of the water-debris thermal exchanges. However, the experimental data are difficult to use due to the failure of several thermocouples (3 of the 5 thermocouples located close to the centre of the vessel and with an elevation up to 10 mm) whose maximum range of temperature is near 1500 K, whereas ASTEC evaluates higher temperatures;
- The temperature of the core catcher: convective heat transfers probably occur in the corium lower layer but are not taken into account in the model.



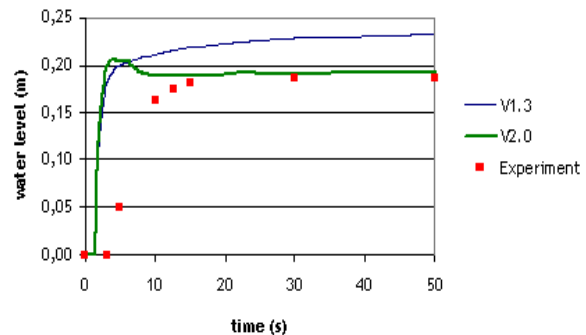
a)



b)



c)



d)

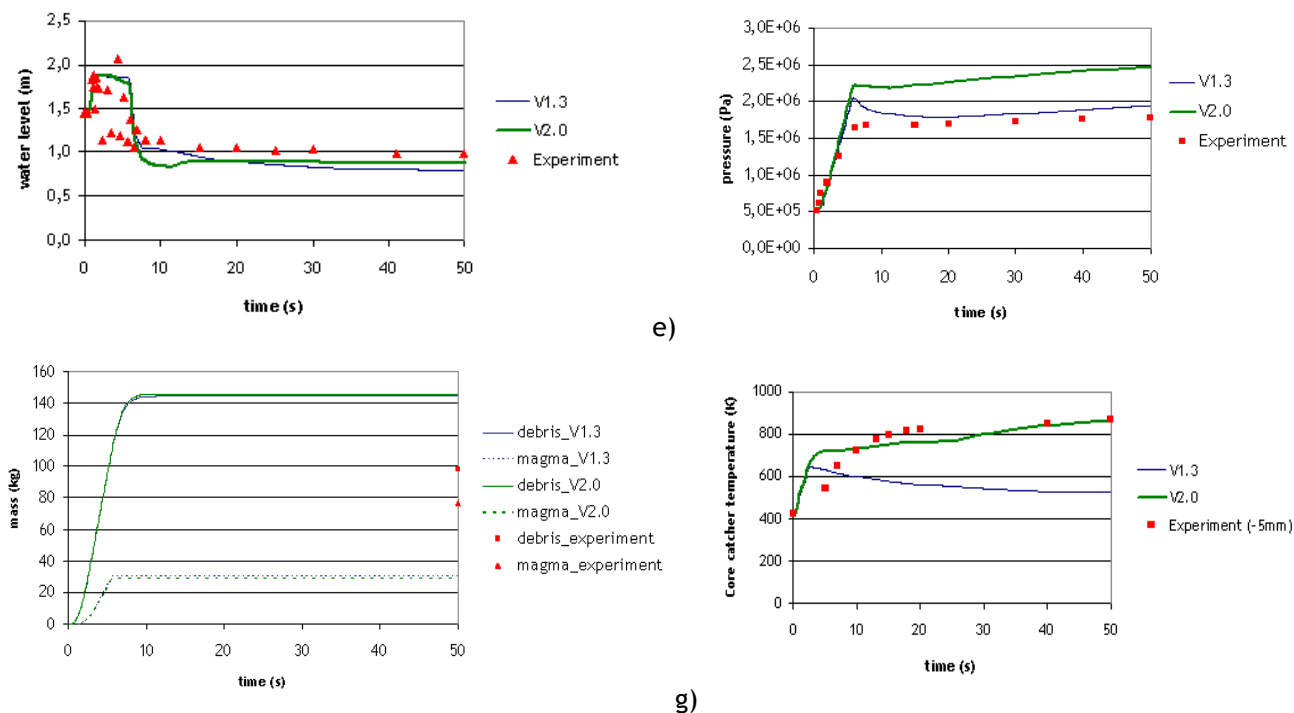


Fig.3 - L28 experiment: a) masses (the melt is named “magma”), b) pressure history, c) inner vessel water level, d) annular vessel water level, e) water temperature, f) steam temperature, g) debris bed temperature, h) core catcher temperature

For the L28 experiment, some differences are observed between V1.3 and V2.0 calculations, in addition to the ones observed in the previous case (concerning the core catcher temperature and already explained). The water level evaluation gives better results than the previous one with the V1.3 version. This could be linked to the improvements implemented in CESAR (compared to V1.3 rev.0) concerning the calculation of the condensation and evaporation in water level volumes. This modification impacts more the L28 calculations than the L14 probably because the initial pressure is 10 times lower in the L28 case, which leads to emphasize the effect of vaporization. This modification also explains the differences obtained for the pressure and water temperature evolutions. However, it leads to overestimate these parameters compared to the experimental results. Possible improvements are investigated in the following section.

Finally, in the calculation, 83% of the corium is fragmented whereas the experimental data is 56%. This discrepancy is difficult to analyse as the nature of the cake obtained at the end of the experiment is questionable. Indeed, it shows a large porosity and agglomeration of particles with the melt (Magallon, 2006), indicating that some fragments were probably not taken into account in the final inventory because they could not be separated from the cake.

3.2. Sensitivity analyses

LIQFDEBR parameter

The parameter LIQFDEBR is the threshold of debris molten fraction for which the liquid part is transferred to the closest corium layer. For the V1.3 validation, this parameter was fixed to 1. Thus this

value was also chosen for the comparison with V2.0 version presented in the section 3.1. This means that debris materials are transferred to a dense corium layer only when they are fully molten. Thus the particles are assumed to start melting in their centre and this molten part is not immediately available to flow towards the corium layer. On the contrary, the value 0 corresponds to the assumption that any amount of molten debris, even small, is able to flow towards the adjacent corium layer. The ASTEC results are presented in Table 2 for LIQFDEBR set to 0 and 1.

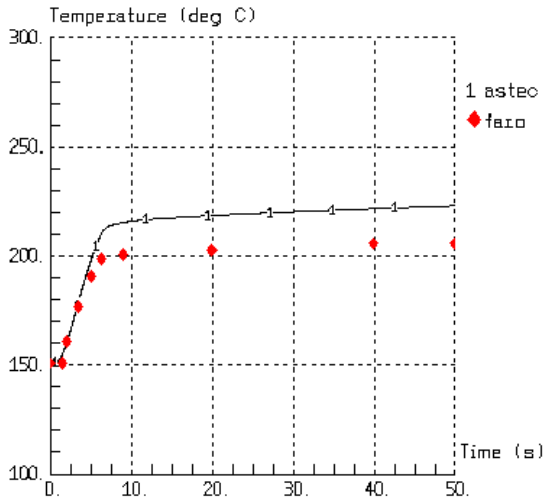
In case of L14 experiment, with the value 0, a significant part of the debris would melt, which reduces the fragmented proportion, in disagreement with experimental results. The sensitivity of L28 calculations to this parameter is low. Therefore, in the current modelling state, it is recommended to set the value at 1: this appears to be conservative for reactor simulations by transferring debris to molten layers when they are totally liquid since partially solid debris in molten layers would lead to decrease the layers temperature.

Table 2: Sensitivity to LIQFDEBR parameter of the fragmented part in L14 and L28 experiments

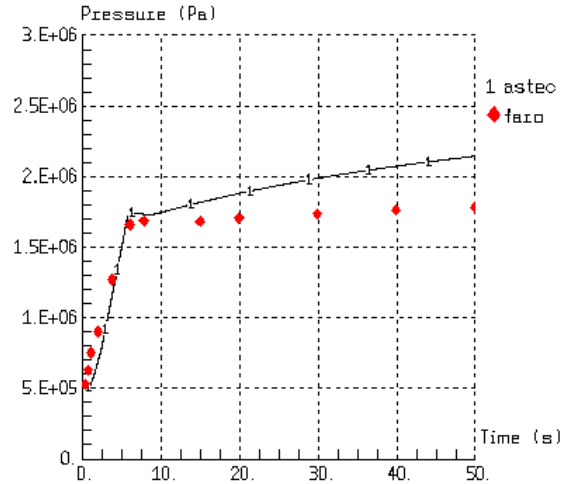
	LIQFDEBR = 1	LIQFDEBR = 0	Experiment
L14	74%	63%	84%
L28	83%	81%	56%

Diameter of debris particles

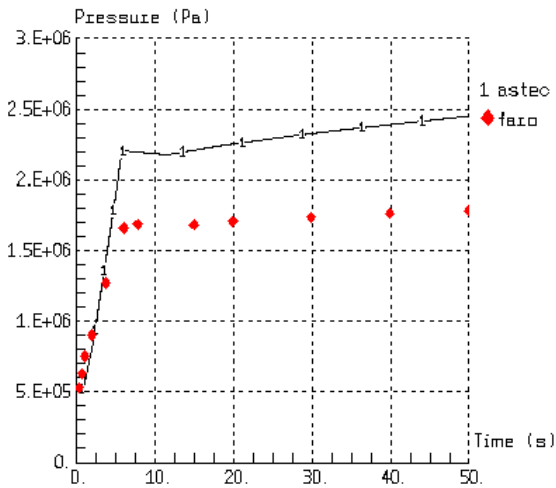
The differences between V1.3 and V2.0 calculations results lead to invalidate the choice of 3 mm for the particle diameter in L28 experiment. In particular, the overestimation of pressure and water temperature suggests to raise the debris diameter. With a debris diameter fixed to 4 mm the results obtained are presented in Fig.4.



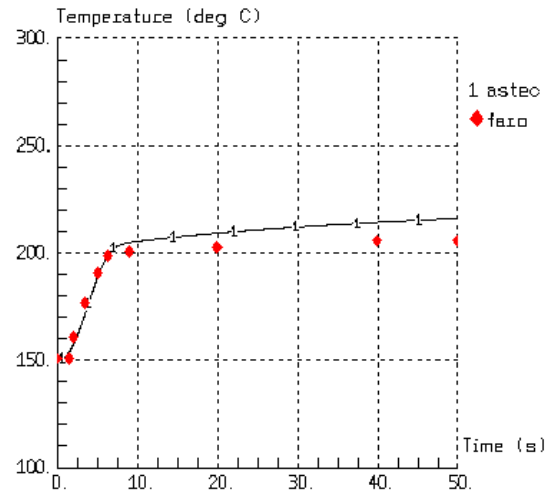
a)



b)



c)



d)

Fig.4 - L28 experiment - Pressure evolution: debris diameter fixed to a) 3 mm, b) 4 mm; Water temperature evolution: debris diameter fixed to c) 3 mm, d) 4 mm.

The increase of the debris diameter improves the pressure evaluation but the slope of the curve remains too sharp compared to the experimental values. Reasons for this discrepancy are investigated in the next Section. This modification also improves the water temperature evaluation (Fig.4 c and d) but does not change significantly the repartition between fragmented and melted parts.

Deep bed heat exchange coefficient

In the simulation of L28 experiment, the pressure increases too sharply compared with the experiment. This could be explained by examination of the distribution of materials at the end of the experiment. It shows that the dense corium is mainly located in the centre of the vessel, whereas debris are mainly located in the annular space around the dense corium (see Fig.5 from Magallon, 2006).

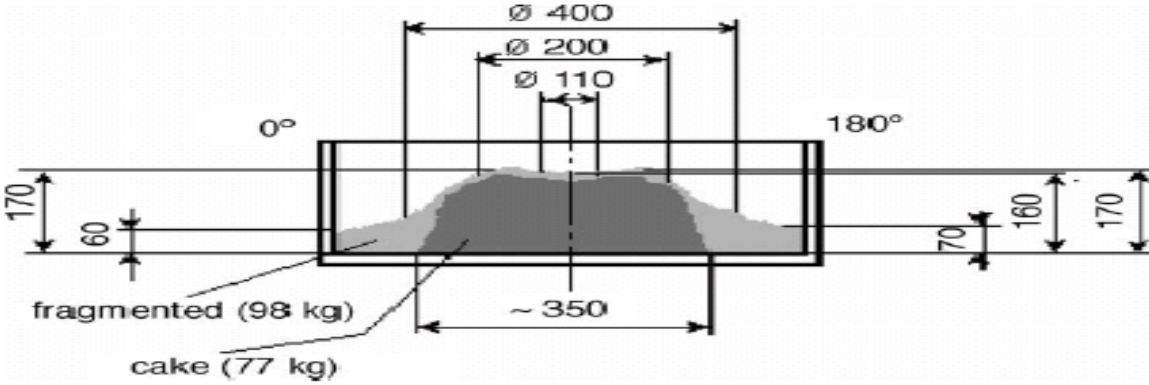


Fig.5 - L28 experiment – Configuration of the debris in the core-catcher

This configuration could be explained by the flow rate of the corium injection which was sufficiently low to allow a good cooling of the corium jet as it flowed down. It was consequently almost solid when it reached the catcher and then was not able to flow along the whole catcher surface. In the calculation, each layer is assumed to be uniformly spread over the vessel surface. This leads to smaller heights for the layers and this underestimation of the debris bed height influences the heat exchanges between the debris bed and water. Indeed, two models are available in ASTEC for the thermal exchanges between fluid and debris bed, depending on the debris bed height. When debris bed height is smaller than 10 cm, the shallow bed model (Dhir, 1983) is used, leading to higher thermal exchanges and consequently higher vaporisation and pressure in the vessel. A new calculation has been performed for the evaluation of the heat exchange coefficient between debris bed and water, considering a modified height and surface for the debris bed according to the experimental results:

$$H_{deb_new} = H_{deb} \times \frac{S_{catcher}}{S_{catcher} - S_{cake}}$$

with H_{deb} being the debris bed height calculated by the code, $S_{catcher}$ the surface of the debris catcher, i.e. the debris bed surface taken into account by the model, and S_{cake} the surface of the non fragmented part of the corium measured after the experiment.

The results of this calculation are presented in Fig.6. These modifications have no significant impact on the water level in the inner vessel and in the annular space, which remain in good agreement with the experimental results.

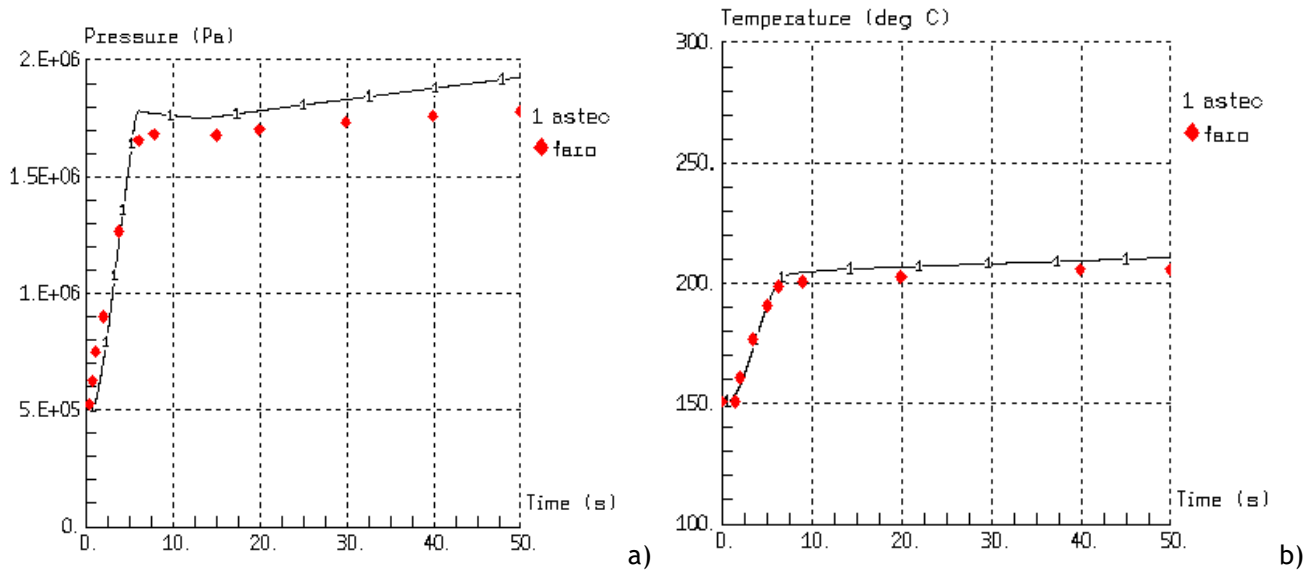


Fig.6 - L28 experiment – a) pressure evolution and b) water temperature evolution: debris diameter fixed to 4 mm and corrected debris bed height and surface

As a conclusion, the ASTEC V2.0 code predictions for corium fragmentation are reasonably good and follow the trends observed in the experiments. However, some limitations in the modelling have been identified and are summarized in the next section.

3.3. Modelling limitations

An important limitation of the predictability of the models used to simulate the corium fragmentation is the necessity to adjust the debris diameter to obtain results close to the experimental values. In the ASTEC code, by default a fixed diameter of 5 mm is considered for the debris. This leads to significant discrepancies with the experimental data, in particular for L14 experiment for which the best-estimate particle size is lower (3.5 mm). The use for L14 experiment of the debris diameter determined for the best-estimate calculation of L28 experiment (4 mm) gives better results. Thus it is recommended to fix the diameter at 4 mm. This is in accordance with the average value, obtained for all FARO tests, of the diameter for which the mass of debris having an upper or lower diameter is equal (see Fig.7 b).

Two correlations are also available for the evaluation of the debris diameter in ASTEC. The most elaborated correlation (Namiech et al., 2004) allows diameter variation during the fragmentation process. In particular, the calculated diameter depends on the jet velocity, the surrounding pressure and temperature, etc. However, the diameter obtained with this correlation is bigger than the one leading to the code best-estimate results on FARO. Thus pressure in the vessel is underestimated, as well as the water temperature and the swollen water level in the annular space. This discrepancy could be explained by the fact that, in Namiech's correlation, secondary fragmentation of the debris is not taken into account. This phenomenon leads to reduce the size of the debris initially formed and therefore to increase the pressure and the water temperature. This deficiency was underlined in Namiech et al. (2004). The second available correlation (Henry et al., 1994) is based on capillary effect and leads to a too small debris diameter (2.4 mm).

In conclusion, the models available in ASTEC to evaluate the debris diameter during fragmentation process depending on thermo-hydraulic conditions do not give best-estimate results for FARO experiments simulations. The use of a fixed diameter, deduced from experimental results, leads to a

better agreement. In case of reactor calculations, the use of this intermediate value in accordance with all FARO tests (see Fig.7 b) allows to reduce the overall error on the energy lost from the corium to the water.

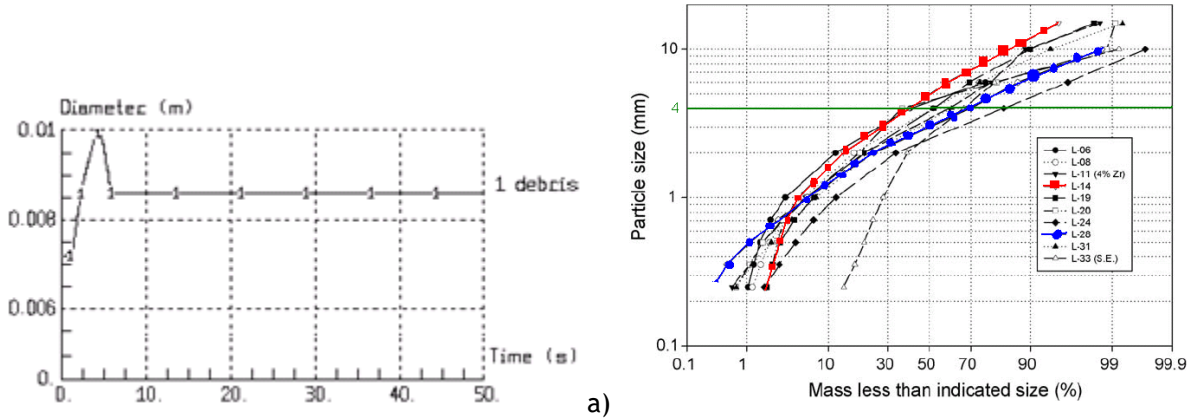


Fig.7 - L28 experiment – a) debris diameter evaluation using Namiech's correlation, b) distribution of the fragmented debris in experiments (from Magallon, 2006)

Another limitation of the modelling concerns the geometry of the layers, which considers that the debris bed or the dense corium are axially equally distributed over the surface of the lower plenum. However, this assumption has a low impact on reactor cases in which shallow bed model is expected to be activated only during short transients.

4. ASTEC VALIDATION VS. LIVE EXPERIMENTS

The LIVE-L1 and LIVE-L6 experiments, performed at KIT (Germany), were designed to study the late phase of core degradation, the formation and stability of crusts and melt stabilization in the reactor pressure vessel by external cooling. In the L6 experiment the configuration with a two-layer melt pool was investigated, with a heated lower layer and an unheated upper layer of molten material. More information about L1 and L6 experiments are available in Miassodov et al. (2008) and Palagin et al. (2012).

For the modelling of the experiments, the molten pool was treated as one homogeneous layer in the L1 experiment and as two layers for the L6 one (for the heated and the unheated parts of the melt). The objective of the validation was to investigate the heat transfer between the corium and the vessel wall. The ASTEC V2 simulations were performed using only the ICARE module in stand-alone. Indeed, the external cooling of the vessel outer wall surface was not modelled but it was simulated in ICARE by using boundary conditions for temperature and heat transfer coefficients at different positions of the vessel wall and derived from the test measurements.

4.1. L1 experiment

The calculated temperature evolution of the layer (T-layer) is compared with the central pool measurements. The fact that only one layer is modelled does not allow to compare with the temperatures profiles in the vessel. However, because of the hemispherical shape of the vessel, the average temperature is close to the value of the thermocouple positioned in the upper part of the melt, which is well predicted by the ASTEC V2.0 version (Fig.8). The difference shown between V1.3 and V2.0

versions is related to a bug correction in the heat exchange coefficient evaluation performed in the last revision of the V2.0 version.

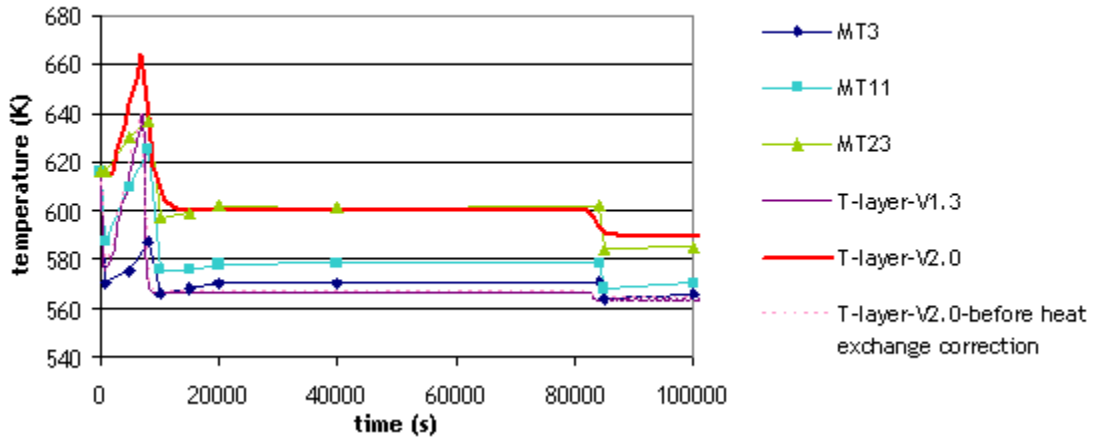


Fig.8 - L1 experiment - Temperature of the melt layer (from bottom to top of the layer: MT3, MT11, MT23)

The best estimated crust thickness profile is calculated choosing a conductivity close to 0.5 W/m/K for the crust (Fig.9). This value is comparable to the value evaluated for the melt conductivity below its liquidus temperature, i.e. 0.46 W/m/K (Buck et al., 2008). The increase of the crust thickness between radius 0.2 and 0.3 is not predicted by the model.

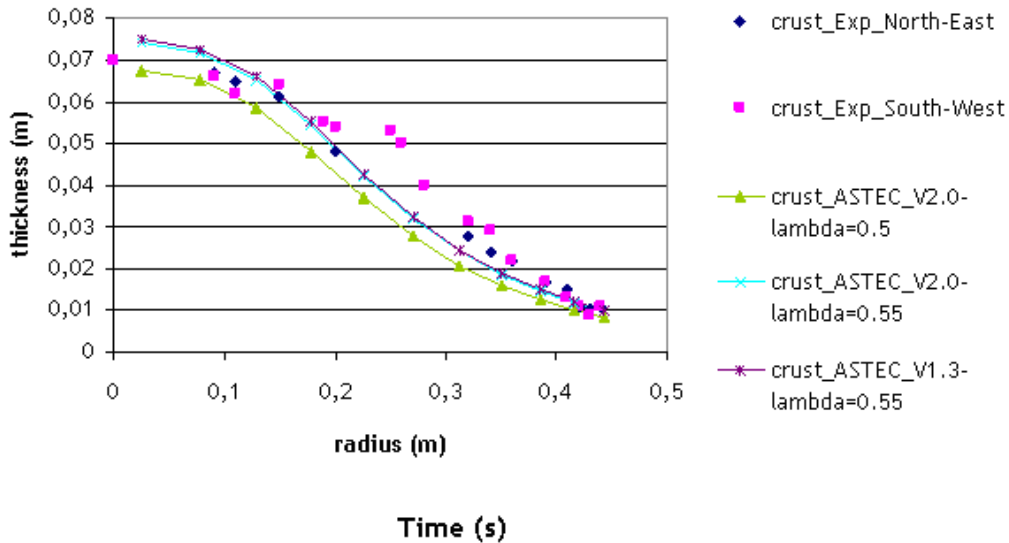


Fig.9 - L1 experiment - Crust thickness profile after melt extraction

4.2. L6 experiment

No study was performed with the V1.3 version for this experiment. With the V2.0 code version, the calculated melt temperature is globally 15 K higher than the measured temperatures. A calculation performed with reduced heating power, to take into account the heat losses due to experimental devices

estimated from experimental results (see Fig.11), leads to a lower discrepancy for the melt temperature between 5 K to 10 K (Fig.10).

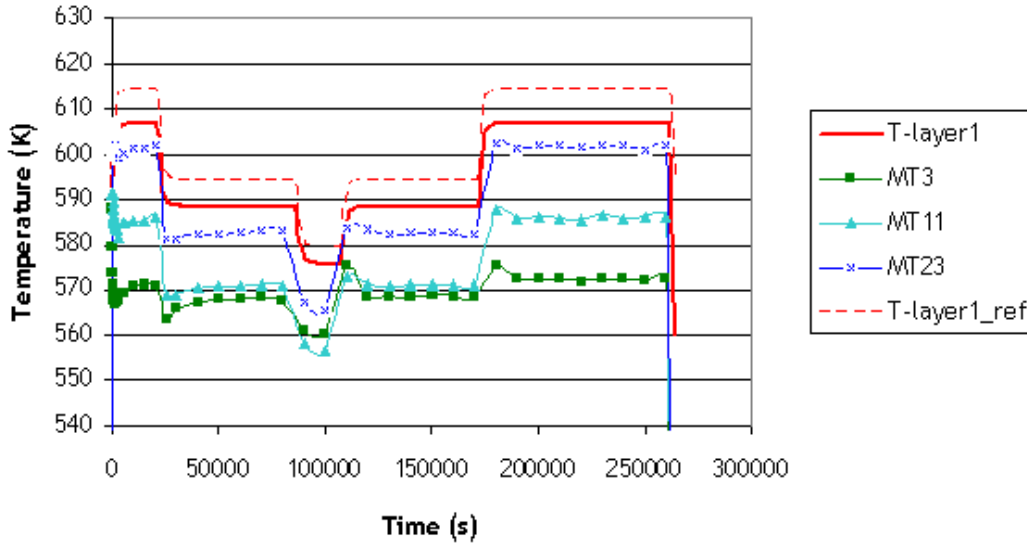


Fig.10 - L6 experiment - Temperature of the lower melt layer with and without reduced heating power

The power distribution between both layers is in agreement with the experimental one (around 20% of the heating power is transmitted from the lower layer to the upper one, see Fig.11).

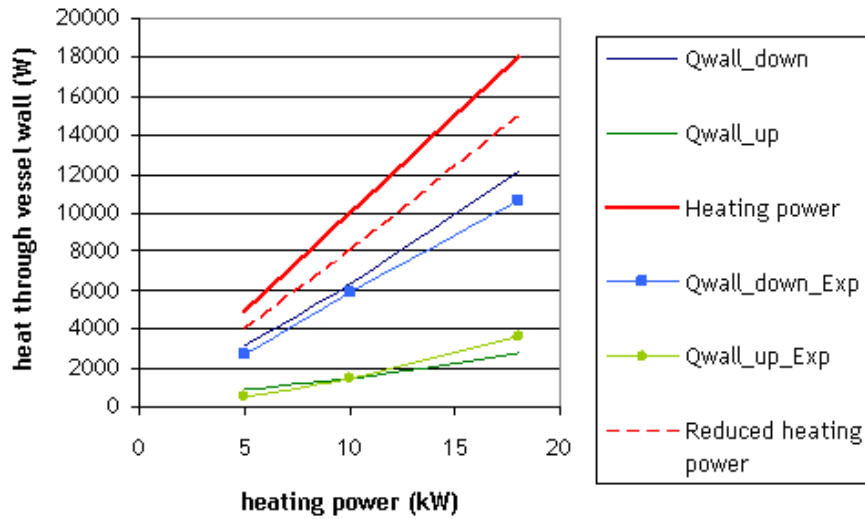


Fig.11 - L6 experiment – Heat transfer through the vessel above (Q_{wall_up}) and below (Q_{wall_down}) the separating plate

The calculated crust thickness at the end of the experiment and during each steady-state phase is in good agreement with the experimental values (Fig.12), taking into account the crust conductivity equal to 0.6 W/m/K, as experimentally measured (see Palagin et al., 2012).

4.3. Modelling limitations

In spite of the fact that, for a melt with homogeneous composition, only one layer with a single temperature is modelled, the ASTEC results obtained in both L1 and L6 experiments show good agreement with experimental values. Similarly, the assumption of steady-state conditions and linear temperature gradient through the crust is satisfying for the validation. However, it should be noticed that, in other configurations, these simplifications could lead to larger uncertainties, particularly when the temperature profile in the layer is sharper or in case of rapid transient leading to strong temperature variations (for the latter, see the CORDEB project in Section 7).

Otherwise, even if it is possible to impose boundaries conditions, a model to simulate the water external cooling appears necessary in particular for reactor calculations. A way could be the coupled use of the modules CESAR and ICARE of ASTEC.

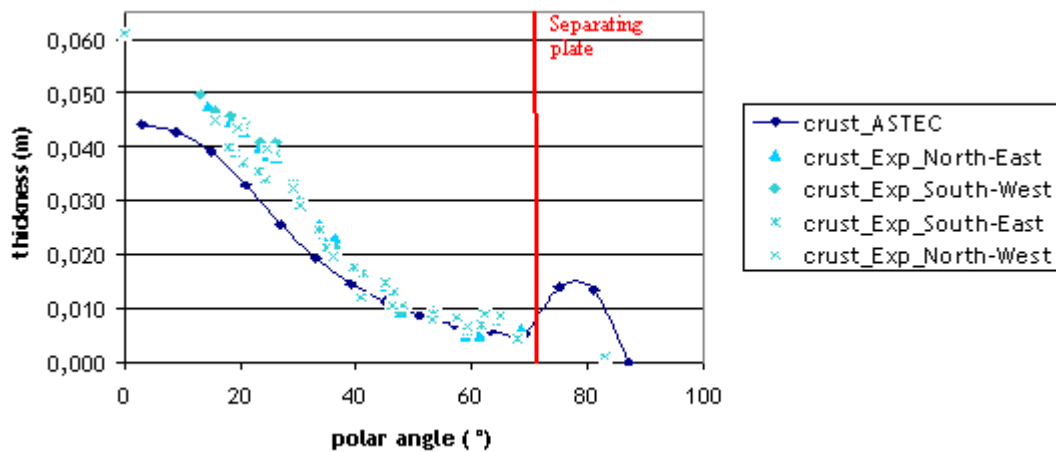


Fig.12 - L6 experiment - Crust thickness profile after melt extraction

5. MASCA EXPERIMENTS

The MASCA series of experiments, performed by NRC-KI (Russia), were designed to study the phase separation of mixtures of UO_2 , ZrO_2 , Zr and Fe/Steel. Some of the experiments also involved fission products simulants, namely Mo, Ru, Sr, Ba, Ce, La, in order to evaluate their re-distribution between the non-miscible phases. For more information, readers may refer to Asmolov et al. (2004), Asmolov and Tsurikov (2007), and Bechta et al. (2008).

The V2.0 version of ASTEC was used to simulate the 21 experiments of the MASCA program: 17 with 0.5 kg of mixture (STFM series) and 4 with 2 kg (MA series). The metal-oxide corium stratification model implemented in ASTEC V2.0 code comes from the one developed for ICARE/CATHARE V2.0 IRSN code (Salay et al., 2005). For all the experiments, the ASTEC V2.0 predictions for corium separation in the presence of structural materials (Fe/Steel) and for fission products distributions are reasonably good and follow the trends observed. The relative errors in metallic mass predictions are on average of 21% for the STFM series (36% maximum) and of 12% for the MA series (21% maximum). Fig.13 depicts the U, Zr and Steel concentrations in the metal phase as a function of relative metal

addition predicted for all experiments involving the corium composed with zirconium being initially oxidized at 32 %. The experimental data trends are well reproduced by the code calculations.

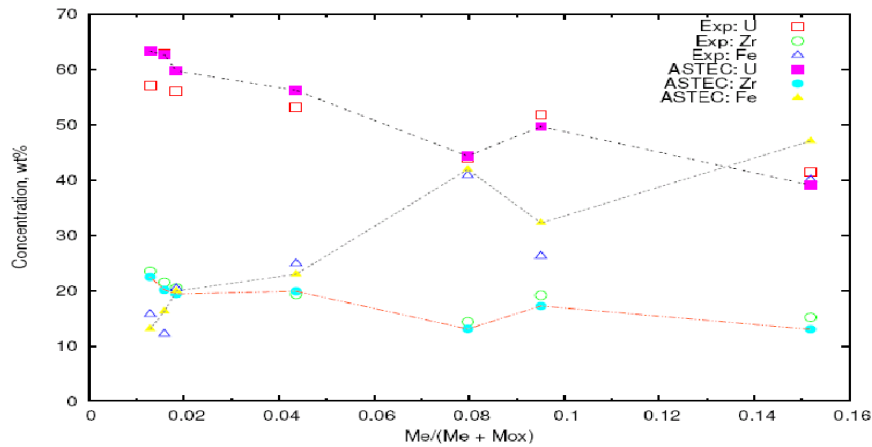


Fig.13 - MASCA experiments - U, Zr and Fe (steel) concentrations for all experiments with 32% initial oxidation of corium zirconium

The limitation of this validation task is the transient behaviour of the separation (the mass transport between the layers is calculated by modelling migration of drops) which could not be assessed due to lack of experimental data. This will need further investigation in the frame of the new CORDEB project (see Section 7).

6. OLHF EXPERIMENTS

The OLHF1 experiment, performed by SNL (USA), intended to simulate the thermal/mechanical loads to a 1/4.85 - scale model of a reactor pressure vessel. This experiment was already included in V1.3 version validation matrix (Koundy et al., 2008) (Bandini et al., 2010). The same modelling was considered for V2.0 calculations. At the inner surface, the imposed temperature boundary conditions correspond to actual experimental measurements. At the vessel outer surface, a constant heat transfer coefficient and a constant ambient temperature condition of 300 K are assumed. The pressure condition inside the vessel is assigned according to the experimental measurements.

The comparison between V1.3 and V2.0 versions did not show any difference. The temperature evolution of the vessel outer surface at two different positions (10° and 70° from the top) is presented in

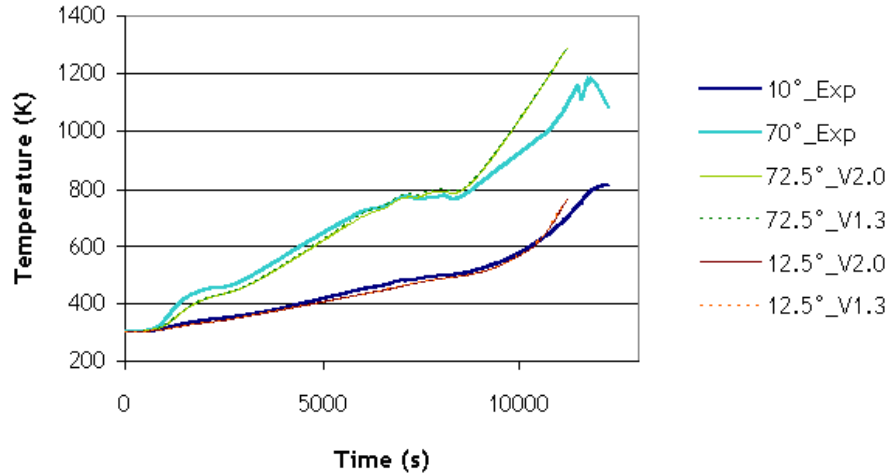


Fig.14. These calculations were performed using the ‘OEUF’ vessel rupture model (Koundy et al., 2008) with the criterion for the vessel rupture corresponding to excessive creep deformation (CRIT = 6). Note that the excessive creep deformation criterion was the one used by default in V1.3 version, whereas all criteria are now checked by default in V2.0 version (CRIT = 0 means that fragile and ductile failure, wall thickness and displacement, creep velocity and deformation are all considered, see Table 3).

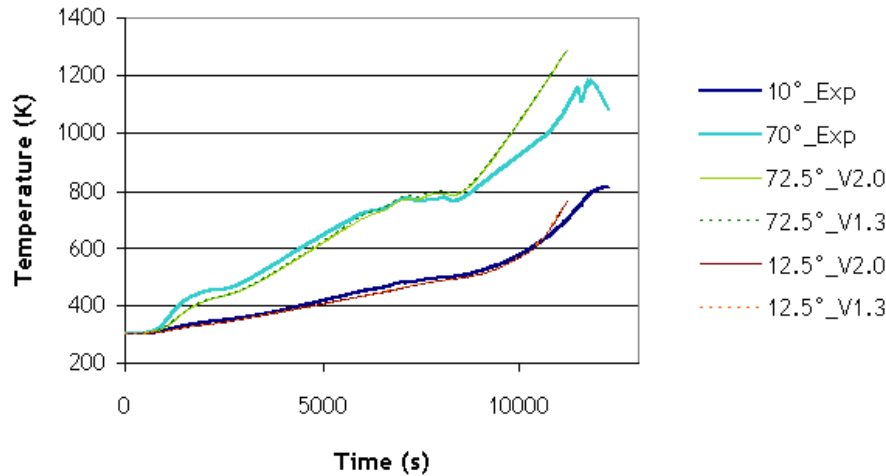


Fig.14 - OLHF1 experiment - Temperature evolution at vessel outer surface (at 10° and 70°) – OEUF model, CRIT = 6

A discrepancy with the experimental results is obtained for the outer vessel temperature at the end of the calculation. This could be linked to the assumption of constant heat transfer coefficient around the vessel surface which is inappropriate: the natural convection flow along the vessel wall would lead to a variable heat transfer coefficient both in time and location. It may also be noted that the current heat transfer model does not take into account the vessel thinning and deformation due to creep.

The elongation value of the vessel as a function of time is presented in Fig.15. The calculated elongation at the end of the curve is close to the experimental one, even if the failure is obtained earlier in the code.

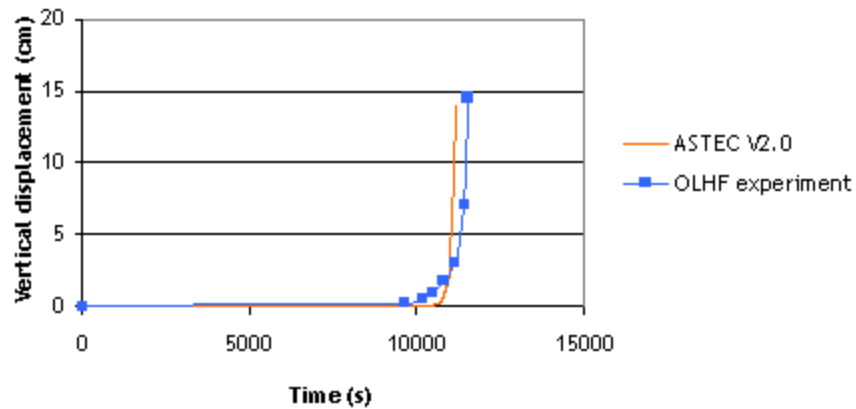


Fig.15 - OLHF1 experiment – Vessel sagging as a function of time – OEUF model, CRIT = 6

The different vessel rupture models available in ASTEC (COMBESCURE, OEUF and LOHEY) have also been tested to evaluate the sensitivity on the time and position of the vessel failure. The results obtained are summarized in Table 3. For the 3 different models, the failure localisations evaluated by the code for the first failure criteria reached (default parameter) are comparable to the experimental one (60° to 75° in the calculations vs. 75° in the experiment) but the rupture time is underestimated from 3% to 13%. As underlined previously, this discrepancy could be linked to the modelling of external heat exchanges around the vessel wall with only one constant coefficient. However, its impact on failure time evaluation is limited.

Table 3 : Rupture time and failure localisation obtained with the different models of V2.0 version

	Type of rupture	Criteria		Time	Location
		Default value	Chosen value		
Experimental results		-		192 min	75°
œUF model					
CRIT 1	Fragile failure	Damage = 1		187 min	65° - 70°
CRIT 2	Ductile failure	Ultimate stress of the material		175 min	60° - 65°
CRIT 3	Too small thickness	0.001 m		187 min	85° - 90°
CRIT 4	Excessive displacement	10 ²⁰ m	0.2 m	187 min	85° - 90°
CRIT 5	Excessive creep velocity	10 ²⁰ s ⁻¹	1 s ⁻¹	187 min	35° - 40°
CRIT 6	Excessive creep deformation	1		186 min	65° - 70°
COMBESCURE model					
CRIT ‘PLASTIC’		Ultimate stress of the material		192,5 min	45° - 60°
CRIT ‘CREEP’		Creep velocity		187 min	60° - 70°
LOHEY model		Creep failure		166 min	65° - 75°

Concerning the OEUF model, the use of criteria 1 and 6, resp. fragile failure and failure due to excessive creep deformation, gives very close results. The ductile failure (criterion 1) is the conservative one in terms of failure time. On the other hand, the criteria 3, 4 and 5 lead to a wrong evaluation of the rupture location. Indeed, these criteria are not designed for a global approach of vessel failure but could be useful for detailed study of a particular case in which maximal values of these criteria would be defined depending on the vessel shape and material properties. That is why default values fixed in the code for these criteria cannot be reached before criteria 1 and 6.

We should note that, both experimentally and numerically, the failure mode is not clearly identified for the OLHF1 experiment. This difficulty was already underlined in the benchmark performed on this experiment with different calculation codes (Nicolas et al., 2003). However, in that case, the rupture times evaluated by ASTEC for the different failure modes are sufficiently close for the simulation of accident scenarios in a reactor. More generally, depending on the accidental scenario, thermal loadings on the lower head vessel could be different and lead to a specific failure mode. Thus, the improvement of thermal loadings evaluation for various transients is an important issue to increase the accuracy of failure time evaluations.

Finally, the crack opening is not modelled in the code and the final size of the hole is not evaluated. However this is an important issue for simulating the melt ejection outside the vessel. Failure propagation is currently investigated by IRSN with a 3D mechanistic code. This work will allow to better understand these phenomena and possibly take them into account in the ASTEC code in the future.

7. CONCLUSION

The ASTEC V2.0 code was assessed by comparison with four series of experiments, each of them dealing with one important phenomenon affecting the corium behaviour in the lower plenum.

The FARO experiments were selected to assess the model of the fragmentation of corium falling into a water pool. Overall, the model may be considered satisfactory for the prediction of the increase of pressure resulting from the interaction with the water and of the fraction of fragmented corium, even if, for L28 test, the mixing of debris and non fragmented corium makes the comparison difficult. As a first step of improvement, it seems necessary to simulate other experiments in order to confirm that the default value used for the debris diameter does not lead to larger uncertainty than the one obtained from the two selected FARO tests. As a second step, it appears that the model would benefit from an improvement of the prediction of the debris size, depending on scenario conditions, in order to provide more accurate initial conditions to the models dealing with the subsequent evolutions of corium (cooling by water, possible melting and chemical interaction).

The LIVE experiments were selected to assess the model predicting the heat transfer between the corium and the vessel wall. The model is considered satisfactory but one has to keep in mind that the experimental conditions are not the most difficult ones to simulate because the Rayleigh number is small (compared to the reactor case) and there is no actual “focusing effect” because the top layer is not “thin” compared to the vessel scale, which prevents a significant increase of the local heat flux in the top layer. So, the model should be assessed by comparison with other experiments in order to cover a wider range of molten pool configurations and intensities of heat flux. Uncertainties in the predicted results are likely to be higher for higher Rayleigh numbers. Moreover, the addition of a model to predict the external cooling of the lower plenum by a coolant flow appears necessary, first, in order to improve the

prediction of boundary conditions for experiments simulations and, mainly to be able to predict the efficiency of external cooling designs at the reactor scale.

The MASCA series of experiments was selected to assess the model predicting the separation of U-Zr-Fe-O corium into non-miscible phases and the subsequent stratification of the molten pool. The model is considered satisfactory in the prediction of the respective masses and compositions of the metallic and oxidic phases. The main limitation of that assessment is that the MASCA experiments were not designed to provide data about the transient behaviour leading to the final stratified state. Therefore, if the final state predicted by ASTEC is considered to be correct, the evolution towards that state remains to be validated (see below the CORDEB project).

The OLHF1 experiment was selected to assess the model predicting the failure of the vessel wall. The model is considered satisfactory despite the relative uncertainty on the timing of failure. Indeed, for a reactor accident scenario, an accuracy of 30 minutes for the time of failure is acceptable because most of the sequences considered for PSA have a duration of several hours. In addition, even for fast sequences, an uncertainty of 30 minutes is comparable to the time necessary for an operator's action, therefore it cannot be considered as significant. In order to be more confident in the consistency of the failure criteria, the assessment should be done with more experimental data. In particular, thermal loading evaluations include uncertainties and various accidental scenarios should be considered. However, the number of available and relevant data is today still limited.

As a general conclusion, it may be underlined that almost all the processes governing the corium behaviour and its thermal interaction with the vessel wall are modelled in ASTEC and that all those models have been assessed individually, with satisfactory results. The main uncertainties appear to be related to the calculation of transient evolutions from one given state (i.e. debris bed following fragmentation) towards another state (i.e. molten pool surrounded by crusts). Only a few experimental data are currently available for such transients, in particular for the time of transition between two states. For example, the RASPLAV-AW-200 experiment (Asmolov et al., 1998) provided data for the transition from a (UO₂-ZrO₂-Zr) debris bed to a molten pool in a lower plenum geometry. The CORDEB programme, which has started recently with new experiments in NITI (Russia), in collaboration with IRSN, EDF and AREVA NP, should also provide relevant data on the corium transient behaviour in the lower head.

REFERENCES

- Asmolov V. G., Abalin S.S., Degaltsev Yu.A., Shakh O. Ya, Dyakov E.K., Strizhov V.F., 1998. Behavior of a core melt pool on the floor of a reactor vessel (RASPLAV Project), Atomic Energy, Vol. 84, N. 4
- Asmolov V. G., Bechta S.V., Khabensky V.B., Gusarov V.V., Vishnevsky V.Yu., Degaltsev Yu.A., Abalin S.S., Krushinov E.V., Vitol S.A., Almjashhev V.I., Kotova S.Yu., Zagryazkin V.N., Dyakov E.K., Strizhov V.F., Kiselev N.P., 2004. Partitioning of U, Zr and FP between molten oxidic and metallic corium, MASCA seminar, Aix-en-Provence, France, June 10-11, 2004. http://www.oecd-neo.org/nsd/workshops/masca2004/oc/papers/RF_M_Partitioning.pdf
- Asmolov V. G., Tsurikov D. F., 2004. MASCA project: major activities and results. MASCA seminar, Aix-en-Provence, France, June 10-11, 2004. http://www.oecd-neo.org/nsd/workshops/masca2004/oc/papers/RF_ASM_M_Activities.pdf
- Asmolov V. G., Zagryazkin V. N., Tsurikov D. F., 2007. The thermodynamics of U-Zr-Fe-O Melts. Thermophysical properties of materials, High Temperature, Vol. 45, N°3, 305-312.

Bandini G., Buck M., Hering W., Godin-Jacqmin L., Ratel G., Matejovic P., Barnak M., Paitz G., Stefanova A., Trégourès N., Guillard G., Koundy V., 2010. Recent advances in ASTEC validation on circuit thermal-hydraulic and core degradation. *Progress in Nuclear Energy*, Volume 52, Issue 1, 148-157.

Bechta S.V., Granovsky V.S., Khabensky V.B., Gusarov V.V., Almiyashev V.I., Mezentseva L.P., Krushinov E.V., Kotova S.Yu., Kosarevsky R.A., Barrachin M., Bottomley D., Fichot F., Fischer M., 2008. Corium phase equilibria based on MASCA, METCOR and CORPHAD results. *Nuclear Engineering and Design*, 238 (10), 2761-2771.

Buck M., Burger M., Gaus-Liu X., Palagin A., Godin-Jacqmin L., Tran C.T., Ma W.M., Chudanov V., 2008. The LIVE program: test and joint interpretation within SARNET and ISTC, *Proceedings of the 3rd European Review Meeting on Severe Accident Research (ERMSAR 2008)*, Nessebe, Bulgaria, September 23–25, 2008.

Dhir V.K., 1983. On the coolability of degraded LWR cores. *Nuclear Safety*, 24(3):319–337.

Henry R.E., Hammersley R.J., Klopp G.T., and Merilo M., 1994. Experiments on the lower plenum response during a severe accident. In *4th International Topical Meeting on Nuclear Reactor Thermal Hydraulics (NURETH-4)*.

Koundy V., Fichot F., Willschuetz H.G., Altstadt E., Nicolas L., Lamy J.S., Flandi L., 2008. Progress on PWR lower head failure predictive models. *Nuclear Engineering and Design* 238, 2420-2429.

Magallon D., Hohmann H., 1997. Experimental investigation of 150-kg scale corium melt quenching in water. *Nucl. Eng. Des.* 177, 321–337.

Magallon D., 2006. Characteristics of corium debris bed generated in large-scale fuel-coolant interaction experiments. *Nuclear Engineering and Design* 236, 1998–2009.

Miassoedov A., Cron T., Foit J., Gaus-Liu X., Schmidt-Stiefel S., Wenz T., 2008. LIVE experiments on melt behaviour in the RPV lower head. *Proceeding of the 16th International Conference on Nuclear Engineering (ICONE16)*, Orlando, USA, May 11-15, 2008.

Namiech J., Berthoud G., Coutris N., 2004. Fragmentation of a molten corium jet falling into water. *Nuclear Engineering and Design* 229, 265-287.

Nicolas L., Durin M., Koundy V., Mathet E., Bucalossi A., Eisert P., Sievers J., Humphries L., Smith J., Pistora V., Ikonen K., 2003. Results of benchmark calculations based on OLHF-1 test. *Nuclear Engineering and Design* 223, 263–277.

Palagin A., Miassoedov A., Gaus-Liu X., Buck M., Tran C.T., Kudinov P., Carénini L., Koellein C., Luther W., Chudanov V., 2012. Analysis and interpretation of the LIVE-L6 experiment, *Proceedings of the 5th European Review Meeting on Severe Accident Research (ERMSAR 2012)*, Cologne, Germany, March 21–23, 2012.

Salay M., Fichot F., 2005. Modelling of metal-oxide corium stratification in the lower plenum of a reactor vessel. *11th International Topical Meeting on Nuclear Thermal-Hydraulics (NURETH-11)*, Avignon, France, October 2-6, 2005.